

K^+K^- AND $K_S^0K_S^0$ PRODUCTION IN TWO-PHOTON COLLISIONS AT BELLE

H. C. HUANG
(for the Belle Collaboration)

Department of Physics, National Taiwan University, Taipei 106, Taiwan
E-mail: hchuang@phys.ntu.edu.tw.

The production of a kaon pair (K^+K^- and $K_S^0K_S^0$) in two-photon processes has been measured using the Belle detector at the electron-positron collider KEKB. We have obtained the invariant-mass distribution of the processes between 1.3 and 2.3 GeV. A broad bump structure around 1.7 GeV in the $K_S^0K_S^0$ channel is confirmed, while, in the K^+K^- channel, a bump structure is seen near 1.9 GeV. The angular distribution of the final-state kaons is analyzed to explore the spin(-helicity) structure in each invariant-mass region for the two processes. Contributions from existing and postulated resonances are discussed.

1 Introduction

A high-luminosity electron-positron collider is a good place to study meson resonances produced by two-photon collisions. The well established two-photon resonance in kaon-pair final states is the $f_2'(1525)$ meson^{1,2}, which is classified as an almost pure $s\bar{s}$ meson. The L3 Experiment at LEP has also reported a resonance-like peak around 1750 MeV in the $K_S^0K_S^0$ final state².

Meson spectroscopy in the 1.5 – 2.0 GeV region is important since glueballs are expected to be found in this mass range. Glueball candidates around 1.7 and 2.2 GeV have been reported in $J/\psi \rightarrow \gamma K\bar{K}$ decays by the BES Experiment at BEPC³. Glueball searches are complicated by excitations of $q\bar{q}$ mesons that also populate the same region. Since gluons do not couple to photons, the two-photon partial decay widths ($\Gamma_{\gamma\gamma}$) of pure glueball states are expected to be very small. Two-photon processes, therefore, play an important role in the search for glueballs. Indeed, null results from the CLEO Experiment at CESR⁴ lend some support for the glueball interpretation of the $f_J(2220)$, while the L3 result suggests the 1700 MeV region should be studied in further detail.

2 Experiment

The analysis is based on data taken by the Belle detector⁵ at the KEKB⁶ asymmetric e^+e^- collider in the period from October, 1999 to December, 2000. The integrated luminosity of the data set analyzed for K^+K^- final states is 5.86 fb^{-1} and 10.6 fb^{-1} for $K_S^0K_S^0$ final states. Since the beam-energy dependence of two-photon processes is very small, we combine data taken at the $\Upsilon(4S)$ resonance ($\sqrt{s} = 10.58 \text{ GeV}$) with data collected at \sqrt{s} values 50 MeV and 60 MeV lower.

The Belle detector⁵ is a general purpose detector which includes a 1.5 T superconducting solenoid magnet that surrounds the KEKB crossing point. Charged tracks

are reconstructed using an 50-layer Central Drift Chamber (CDC) and a 3-layer double-sided Silicon Vertex Detector (SVD). Particle identification is accomplished by combining the responses from a Silica Aerogel Čerenkov Counters (ACC) and a Time of Flight Counter system (TOF) with specific ionization (dE/dx) measurements in the CDC. A CsI Electromagnetic Calorimeter (ECL) located inside the solenoid coil is used for photon detection and electron identification. Almost all the signal events used in the analysis were triggered by requiring two or more tracks in the CDC.

3 K^+K^- Final States

3.1 Event Selection

Events with only one pair of charged particles produced in two-photon processes ($\gamma\gamma \rightarrow X^+X^-$) are selected with the following criteria: the scalar sum of track momenta ($\sum |p|$) in an event is required to be smaller than 6 GeV/ c , and the sum of the calorimeter energies in an event less than 6 GeV. The event is required to have only one positively charged track and only one negatively charged track, where each satisfies the conditions: $p_t > 0.4 \text{ GeV}/c$, $|dr| < 1 \text{ cm}$, $|dz| < 2 \text{ cm}$, $-0.34 < \cos\theta < 0.82$, where p_t is a transverse momentum of a track with respect to the positron beam axis, and dr and dz are r and z coordinates, respectively. All of the above values are measured in the laboratory frame. A cut on p_t balance in the e^+e^- CM frame, $|\sum \mathbf{p}_t^*| < 0.1 \text{ GeV}/c$, is applied to select exclusive-two-track events from quasi-real two-photon collisions.

We make particle identification cuts for the two tracks to select K^+K^- events. Since the sample included a large fraction of $\gamma\gamma \rightarrow e^+e^-$ events, we reject them by requiring $E/p < 0.8$ for the two tracks, where E/p is the ratio of the energy deposit on ECL to the momentum. Charged kaons are selected using TOF and ACC information with the criteria that the likelihood ratios for K/π and K/p separation are larger than 0.8. In addition,

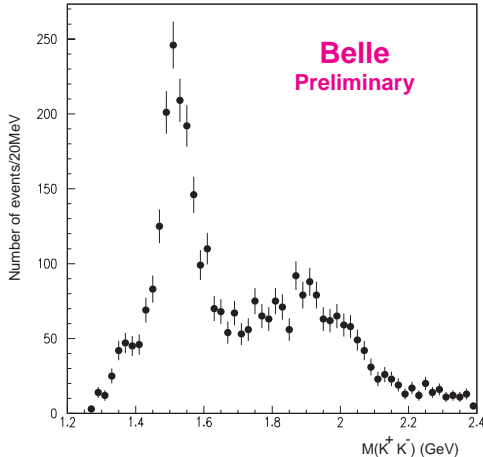


Figure 1: The invariant mass distribution for $\gamma\gamma \rightarrow K^+K^-$ events.

dE/dx information from CDC is also used for identifying kaons in the lowest invariant mass region.

3.2 Invariant Mass Distribution

After the application of all the selection criteria, 3674 events remain. Figure 1 shows the K^+K^- invariant mass distribution for the selected samples. The peak at $1.48 - 1.56$ GeV is from $f_2'(1525) \rightarrow K^+K^-$. In addition, there is a broad bump in the $1.7 - 2.1$ GeV region. No significant enhancement around 2.23 GeV is observed.

The mass region near the $f_J(2220)$ is shown in detail in Figure 2. The signal region is chosen to be within 2220 MeV and 2260 MeV. To obtain the background shape, we fit the K^+K^- mass distribution as a second-order polynomial from the sideband regions. We observed 48 events in the signal region and the expected background is 49.2. Using a Poisson distribution with background, we obtain a 95% C.L. upper limit

$$\Gamma_{\gamma\gamma}(f_J(2220)) \times \mathcal{B}(f_J(2220) \rightarrow K^+K^-) < 1.5eV$$

under the assumption of $(J, \lambda) = (2, 2)$.

3.3 Analysis of the Angular Distribution

We made a model-independent partial-wave analysis for the angular distribution of the K^+K^- events. For the total angular momentum (J) of the $\gamma\gamma$ system, we assumed that partial waves with $J \geq 4$ were negligible. The odd- J waves are forbidden by the symmetric nature of the initial state and the parity conservation. In the $\gamma\gamma$ system, the differential cross section can be written as

$$\frac{d\sigma}{d\Omega} = |\mathcal{H}(J=0, \lambda=0) + \mathcal{H}(J=2, \lambda=0)|^2 + |\mathcal{H}(J=2, \lambda=2)|^2 \quad (1)$$

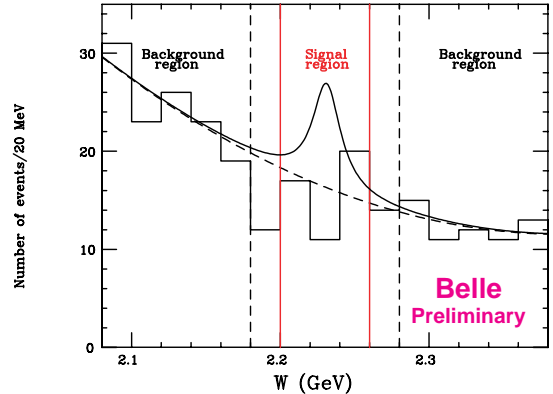


Figure 2: K^+K^- mass distribution (GeV) observed in data near the $f_J(2220)$ mass. The background shape (dashed line) is assumed to be a second-order polynomial. The solid line is the sum of a fit to the background and the signal line shape for central values of the resonance parameters, $M_{f_J} = 2.231$ GeV and $\Gamma_{f_J} = 23$ MeV, corresponding to the observed 95% C.L. upper limit of 14.7 excess events.

where the \mathcal{H} 's are the partial-wave amplitudes for the J and λ (helicity) states.

Equation (1) includes four real-number parameters, the sizes of the three partial wave amplitudes and one relative phase between the two $\lambda = 0$ waves. Expressing Eq. (1) with d -functions, the angular distribution can be reduced to

$$\frac{d\sigma}{d|\cos\theta^*|} = \mathcal{X} + \mathcal{Y}|d_{00}^2(\cos\theta^*)|^2 + \mathcal{Z}|d_{20}^2(\cos\theta^*)|^2 \quad (2)$$

Here the three parameters \mathcal{X} , \mathcal{Y} and \mathcal{Z} can be written in terms of the three partial-wave amplitudes and one relative phase, as explicitly presented in the Reference⁷. However, in Eq. (2), we still cannot determine \mathcal{Y} and \mathcal{Z} independently, since the two d -functions have a similar shape for $|\cos\theta^*| < 0.5$. Therefore, we introduced two new parameters, $\mathcal{Z}' = \mathcal{Y} + \mathcal{Z}$ and $f = \mathcal{Y}/\mathcal{Z}$, and assumed $f = 0.5$. The fitting results for \mathcal{X} and \mathcal{Z}' are not sensitive to the choice of the f value. The parameter \mathcal{X} contains the $J = 0$ cross section dominantly, whereas the parameter \mathcal{Z}' is dominated by the $J = 2$ contributions, if the contribution of the interference effect between the two $\lambda = 0$ states are sufficiently small.

We have fit the \mathcal{X} and \mathcal{Z}' values at different W points independently. Figure 3 shows the W dependences of the parameters (we give the results in $\mathcal{Z}'/5$ to normalize them to the contribution in the total cross section). It is clear that the two peak structures from $f_2'(1525)$ and of 1.9 GeV region are dominated by $J = 2$ components. The $J = 0$ component is consistent with zero except in the highest W region.

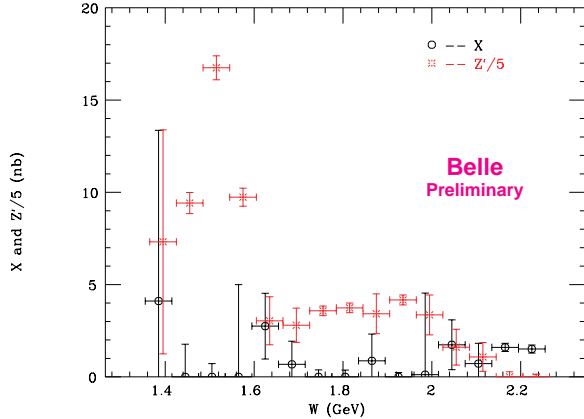


Figure 3: The contribution to the total cross section from the components \mathcal{X} (dominated by $J = 0$, open circles) and $Z'/5$ (dominated by $J = 2$, asterisk marks).

4 $K_S^0 K_S^0$ Final States

4.1 Event Selection

Only events where both K_S^0 's decay to $\pi^+ \pi^-$ are considered. To select events in which the K_S^0 's were produced in two-photon collisions, we require that: the scalar sum of track momenta ($\sum |p|$) in an event is smaller than 6 GeV; the sum of calorimeter energies in an event is smaller than 6 GeV; there are exactly four reconstructed charged tracks with a net charge of zero; and the total momentum imbalance in the transverse plane satisfies $P_t^2 \equiv |\sum \mathbf{p}_t^*|^2 < 0.1 \text{ GeV}^2$, to select events with small incident photon virtuality.

The charged tracks are assumed to be pions. A pair of oppositely charged tracks are combined to form a K_S^0 candidate if their reconstructed vertex is displaced from the primary interaction vertex. The tracks are then re-fit with the constraint that they come from the reconstructed vertex. They are kept if the resulting invariant mass for the pair is within 10 MeV of M_{K^0} ⁸ and the combined momentum vector points back to the interaction vertex. After these selection cuts, the mass resolution is obtained to be 2.6 MeV. The pairs are again fit, constraining the mass of each K_S^0 candidate to the nominal PDG value⁸.

Since the two K_S^0 's are produced back-to-back in the transverse plane, the angle between the flight directions of the two K_S^0 candidates in this plane is required to be larger than 160° . A legoplot of the two unconstrained pion-pair masses is shown in Figure 4. There is a strong enhancement at $(m_{K_S^0}, m_{K_S^0})$ and the background fraction is very low. After applying all the selection cuts, 1511 events are found in the data sample.

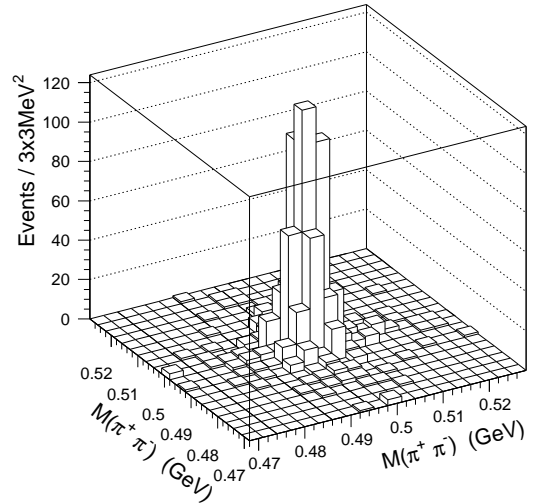


Figure 4: $m_{\pi^+ \pi^-}$ of one K_S^0 candidate versus $m_{\pi^+ \pi^-}$ of the other. There is a strong enhancement near the $(m_{K_S^0}, m_{K_S^0})$ point over a very small background.

4.2 Analysis

The resulting $K_S^0 K_S^0$ invariant mass spectrum is shown in Figure 5. The spectrum obtained is similar to the one reported by the L3 Experiment². The spectrum is dominated by the $f_2'(1525)$ resonance and a clear enhancement is visible in the 1750 MeV region. The $f_2(1270) - a_2^0(1320)$ region shows the destructive interference expected in the $K_S^0 K_S^0$ final state⁹. The event rate in this region is suppressed by the detection efficiency.

The $K_S^0 K_S^0$ invariant mass spectrum is fitted by minimizing a χ^2 function for the expected value in the i th bin.

$$E_i = \xi_i \cdot (G_i + BW_i^{(1)} + BW_i^{(2)} + B_i). \quad (3)$$

where ξ_i is the detection efficiency parameterized from the Monte Carlo. The small bump in the $f_2(1270) - a_2^0(1320)$ region is described by a Gaussian function G_i with its mean and sigma as free parameters. The peaks at $f_2'(1525)$ and 1750 MeV regions are described by Breit-Wigner functions BW_i with their masses and widths taken as free parameters. The background is assumed to be a constant (B_i) in the fit. The result of the fit is illustrated by the curve in Figure 5. The parameters obtained are summarized in Table 1.

4.3 The $f_J(2220)$ Mass Region

No enhancement at the $f_J(2220)$ mass is observed. We assume a mass of 2230 MeV and a total width of 20 MeV. The signal region is chosen to be ± 40 MeV around 2230

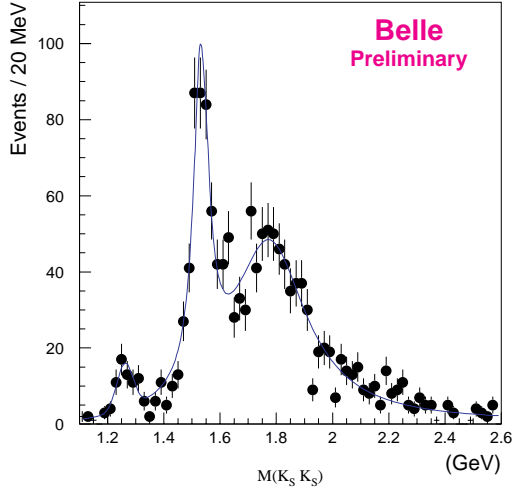


Figure 5: The $K_S^0 K_S^0$ invariant mass spectrum for the $\gamma\gamma \rightarrow K_S^0 K_S^0$ process. The solid line is a fit with two Breit-Wigner functions for the $f_2'(1525)$ and 1750 MeV region, and a Gaussian for the $f_2(1270) - a_2^0(1320)$ region plus a constant background. See the text for details.

Table 1: Results of the fit to the $K_S^0 K_S^0$ mass spectrum.

	$f_2'(1525)$	1750 MeV
Mass (MeV)	1532 ± 4	1768 ± 9.6
Width (MeV)	64 ± 6.8	323 ± 29
No. of Events	414 ± 36	967 ± 72

MeV. To obtain a background shape, we fit the $M_{K_S K_S}$ distribution with a linear function from 2.11 to 2.35 GeV, excluding the signal region. We observed 36 events in the signal region and the expected background is 27.0. Using a Poisson distribution with background, we obtain an upper limit of 20.7 signal events at the 95% C.L. Assuming $(J, \lambda) = (2, 2)$ for $f_J(2220)$, this corresponds to

$$\Gamma_{\gamma\gamma}(f_J(2220)) \times \mathcal{B}(f_J(2220) \rightarrow K_S^0 K_S^0) < 1.17\text{eV}$$

at 95% C.L. without considering the systematic errors.

4.4 Angular Analysis

We have applied the same method of partial wave analysis, described in Sec. 3.3, to the $K_S^0 K_S^0$ data sample. The angular distribution of each W bin is fit by Eq. 2. Figure 6 shows the W dependences of the fitted results, $\mathcal{Z}'/5$ and \mathcal{X} , which correspond to the contribution of $J = 2$ and $J = 0$ components in the total cross section, respectively. It is clear that the peak of $f_2'(1525)$ is dominated by spin-2 component as expected. However, there is a

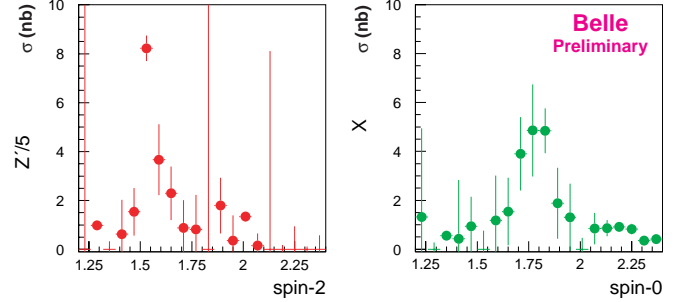


Figure 6: The contribution to the total cross section from the components (a) $\mathcal{Z}'/5$, dominated by spin-2 component, and (b) \mathcal{X} , dominated by spin-0 component.

large spin-0 component in the 1750 MeV region while some spin-2 structure appears around 1.8 – 2.0 GeV.

5 Summary

We have studied the reactions $\gamma\gamma \rightarrow K^+ K^-$ and $\gamma\gamma \rightarrow K_S^0 K_S^0$ using the large data samples collected by the Belle experiment at KEKB. A prominent $f_2'(1525)$ resonance is observed in both channels. A broad structure in the 1.7–2.1 GeV region is found in $K^+ K^-$ and an enhancement around 1750 MeV is observed in $K_S^0 K_S^0$. A partial wave analysis has been performed to explore these resonance structures. Upper limits for $f_J(2220)$ are also obtained in both channels, respectively.

References

1. TASSO Collaboration, M. Althoff *et al.* Phys. Lett. **121B** (1982) 216; PLUTO Collaboration, Ch. Berger *et al.* Z. Phys. **C37** (1988) 329; and CELLO Collaboration, H.J. Behrend *et al.* Z. Phys. **C43** (1989) 91.
2. L3 Collaboration, M. Acciarri *et al.*, Phys. Lett. **B363** (1995) 119; *ibid.* **B501** (2001) 173.
3. BES Collaboration, J.Z. Bai *et al.*, Phys. Rev. Lett. **76** (1996) 3502; **77** (1996) 3959.
4. CLEO Collaboration, R. Godang *et al.*, Phys. Rev. Lett. **79** (1997) 3829; M.S. Alam *et al.*, *ibid.*, **81** (1998) 3328.
5. The Belle Collaboration, A. Abashian *et al.*, KEK Progress Report 2000-4, to be published in Nucl. Instr. Meth. A.
6. *KEKB B-Factor Design Report*, KEK Report 95-7, June 1995.
7. VENUS Collaboration, F. Yabuki *et al.*, J. Phys. Soc. Japan **64** (1995) 435.
8. Particle Data Group, D.E. Groom *et al.*, Eur. Phys. J. **C15** (2000) 1.
9. H.J. Lipkin, Nucl. Phys. **B 7** (1968) 321.